

Proportional Integral and Fuzzy Logic Based Voltage and Frequency Controller for Isolated Asynchronous Generator

Sachin Tiwari¹, Rahul Singh², and Suchi Mishra³

^{1,2}Department of Electrical & Electronics Engineering, Lakshmi Narain College of Technology Excellence Bhopal, India, sss.rahulsingh@gmail.com, sachintbpl@gmail.com

³Department of Electronics & Instrumentation, SATI, Vidisha, India, mishrasuchi08@gmail.com,

Abstract— Self-excited induction Generators, often known as SEIGs, are rising in popularity to produce electrical power and provide it in more isolated and rural regions. The cheap cost, stiffness, compact size, and brushless design of SEIGs with distinct excitation banks contribute to their high level of efficiency. The SEIG, on the other hand, has weak voltage and frequency controls. In order to mitigate these drawbacks in response to a wide range of load situations, the constant power SEIG system has an Electronic Load Controller (ELC) linked to it. The classic proportional-integral (PI) controller used for ELC is contrasted with a fuzzy logic-based SEIG-ELC control method in this article. The electronic load cell is made up of a resistor serving as a dump load and an insulated gate bipolar transistor (IGBT)--based chopper switch in a current-controlled voltage source inverter (CC-VSI). The suggested ELC is constructed and replicated in MATLAB using a variety of electrical load circumstances, and their in-depth comparison with the Proportional Integral controller-based ELC system is explored in considerable length. The varied findings illustrate the efficacy of the suggested method under both nonlinear and linear load circumstances, in addition to its superiority when compared to the PI-based SEIG-ELC system.

Keywords— *Electronic load controller, voltage and frequency control, Proportional Integral Controller (PI), Fuzzy logic controller, Self-excited Induction Generator*

1. INTRODUCTION

The production of electrical power is an essential component of the modern global economy. The rapid depletion of fossil fuels and other negative ramifications of environmental deterioration have resulted in the development of alternative and renewable sources of energy. These concerns have arisen in recent years in response to growing awareness of environmental problems such as global warming. Wind, hydro, and solar energy are among the most renowned forms of renewable energy technologies, and they are also among the ones that are growing at the quickest rate. Solar and wind energy sources are still behind the curve because of their reliance on constantly shifting atmospheric conditions. Hydroelectric power plants, on the other hand, are quickly being recognized as an effective alternative that is readily accessible even in geographically inaccessible and isolated

places. Self-excited induction generators (SEIGs) with their own separate excitation banks are proving to be an efficient option for the generation and distribution of electrical energy in remote areas such as rural villages, islands, and hilly terrains. These types of areas experience the absence of a grid and difficulty in the supply of electricity. In order to generate energy at these remote locations, a steady power input, such as that provided by a small, micro, or pico-hydro turbine, is often used to power the SEIG. When it comes to the amount of energy that may be saved, induction generators beat out their synchronous counterparts [1]. This is due to the fact that induction generators are more robust, have brushless construction, are more cost-effective, need minimal maintenance, have a self-protection feature, and do not need DC excitation. However, the most significant drawbacks of SEIG are inadequate frequency and voltage restrictions, in addition to problems with power quality [7]. Because of this, a considerable amount of research and studies have been carried out in the creation of frequency and voltage controllers for purposes that need constant power, constant speed, as well as variable power and speed [2-6]. In order to regulate the voltage and the frequency of systems that require uninterrupted power an ELC is attached across the SEIG, including those that exist in hydropower plants. This connection is made in order to control the frequency and voltage of these applications. The ELC and its control systems have been approached from a variety of angles, each of which has been well described. Most of these are assembled on hysteresis control employing PID control or PI controls, which are both simple to build and involve a lesser level of complexity [8]. Hysteresis control employs proportional-integral-derivative (PID) or proportional-integral (PI) controls. In order to produce schemes for Pulse Width Modulation (PWM) that are delivered to the CC-VSI, this work aims to present a control system that uses fuzzy logic control and combines hysteresis current management. The control scheme will additionally depend on the fuzzy logic control technique and will be focused on the fuzzy logic control technique. The hysteresis current control technique is the specific topic of investigation for this paper. The suggested ELC and its control methods are investigated and contrasted against the PI-based

controller for the SEIG-ELC system, which operates in the same load situations and within the same nonlinear and linear load circumstances.

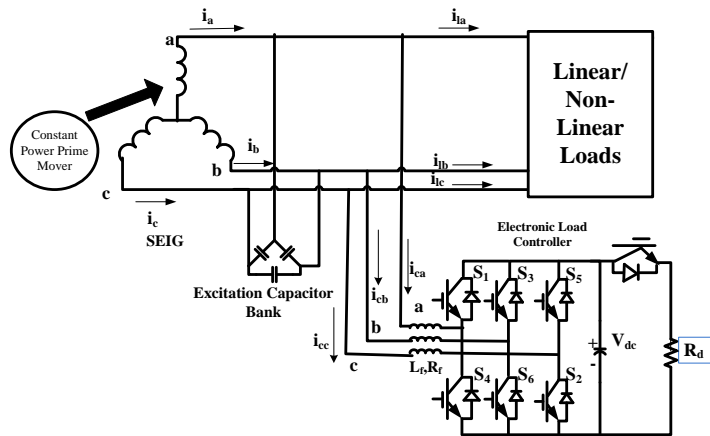


Figure.1. A solitary self-excited induction generator's schematic diagram

I. SYSTEM CONFIGURATION

System setups of each of these approaches are comparable; the only significant difference is in the control mechanism for the ELC. A three-legged CC-VSI with an IGBT-based series resistor and chopper switch that acts as the dump load is the ELC that is recommended to be used for a self-excited squirrel cage induction motor that is operating as an induction generator with a delta-connected fixed capacitor bank. The induction generator is being run in conjunction with a delta-connected static capacitor bank. It is crucial that the capacitor bank be there in order to provide the SEIG with no load excitation. It is important for the functioning of ELCs to run smoothly and continuously, thus careful consideration must be given to the design of both the dump load and the chopper switch. Through the filter circuit, the controller is linked up at the PCC, which stands for the point of common coupling. An appropriate capacitor is placed across the output of the rectifier so that the ripples in the rectifier output voltage may be smoothed out. The chopper switch is made out of an IGBT, and its gate driver circuit was constructed using the fuzzy logic approach. This circuit makes certain that the chopper switch is only triggered if the load on the generator is far a lesser amount of than its rated value. When it comes to the CC-VSI, the hysteresis current controller is the component that is in charge of managing the gate pulses. The hysteresis control has a number of advantages, including the speed with which it responds to load changes and line transients as well as the fact that it is inherently linear. The functioning of ELCs based on fuzzy logic controllers and proportional integral controllers is simulation and modeling in MATLAB using Simulink under a number of different linear and nonlinear load scenarios. The results of these simulations are compared and contrasted. As a consequence of this, it has been shown that

the proposed fuzzy logic controller is able to manage not only the voltage but also the frequency, in addition to being able to fulfill the tasks of volatile power adjuster and load leveler [11].

2. ALGORITHM CONTROL

The equations of working that need to be followed for the control system are as follows:

A. Control for CC-VSI

On the MATLAB platform, a number of control equations are available for the currently controlled voltage source inverter control, which may be used for voltage and frequency control:

1) The inphase component of the reference source current

In order to provide both the auxillary load (Rd) or the consumer load for the purposes which require uninterrupted power, SEIG should produce active power. The in-phase of the current that comes from the reference source is adjusted such that it is equivalent to the specified magnitude of the active power module of the current that comes from the constant power input. This is determined by the following equation:

$$I_{smd}^* = \sqrt{2}(P_{rated})/\sqrt{3}(V_{rated})$$

(1)

where symbols Prated and Vrated stand for the power and voltage, respectively, at their rated levels. Since the instantaneous line voltages at the terminals of SEIG where the phase supply (v_{sa} , v_{sb} , and v_{sc}) are located are considered sinusoidal, the amplitude of these voltages may be determined as follows:

$$V_t = \{ (2/3) (v_{sa}^2 + v_{sb}^2 + v_{sc}^2) \}^{1/2}$$

(2)

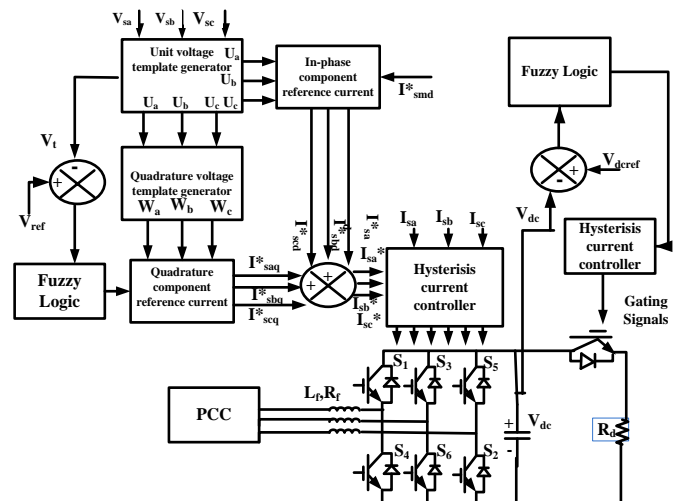


Fig.2. Control strategy for electronic load controller with fuzzy logic controller presented in the form of a schematic design for SEIG

Applying the subsequent formula, it is feasible to calculate simultaneous values of unit amplitude prototypes that are in step through simultaneous voltage (v_{sa} , v_{sb} , and v_{sc}):

$$u_a = v_{sa}/V_t; u_b = v_{sb}/V_t; u_c = v_{sc}/V_t \quad (3)$$

It is possible to estimate the immediate values of the in-phase constituents of the Reference Source Current as:

$$i_{sad}^* = I_{smd}^* u_a; i_{sbd}^* = I_{smd}^* u_b; i_{scd}^* = I_{smd}^* u_c \quad (4)$$

a). Reference source current quadrature component

It is possible to make an approximation of the immediate quadrature components of reference source currents as:

$$i_{saq}^* = I_{smq}^* w_a; i_{sbq}^* = I_{smq}^* w_b; i_{scq}^* = I_{smq}^* w_c \quad (5)$$

where w_a, w_b and w_c are an additional set of unit vectors that have a phase change of ninety degrees following the analogous unit vectors u_a, u_b and u_c whose are supplied in the following manner:

$$w_a = -u_b/\sqrt{3} + -u_c/\sqrt{3} \quad (6)$$

$$w_b = \sqrt{3}u_a/2 + (u_b - u_c)/2\sqrt{3} \quad (7)$$

$$w_c = -\sqrt{3}u_a + (u_b - u_c)2\sqrt{3} \quad (8)$$

1) Reference source current

When calculating the overall reference source currents, the synchronous and quadrature elements of the overall reference source currents are summed simultaneously.

$$i_{sa}^* = i_{sad}^* + i_{saq}^* \quad (9)$$

$$i_{sb}^* = i_{sbd}^* + i_{sbq}^* \quad (10)$$

$$i_{sc}^* = i_{scd}^* + i_{scq}^* \quad (11)$$

b). DC Bus Control for the Chopper Circuit

2) DC link voltage

Following is an equation that will be utilized to determine the DC link voltage:

$$V_{dc} > 2\sqrt{2} (V/\sqrt{3})/mi \quad (12)$$

wherever the modulation index, or mi , is considered to be 1. The estimated value of 677 V is rounded up to the next whole number, which is taken as 700 V for the value of V_{dc} .

3) DC link capacitor

Both the unrestrained rectifier and the helicopter switch have an identical voltage evaluation, which will be decided by the root-mean-square (rms) measurement of the alternating current (ac) the mean of the direct current final voltage, and the supply voltage. The input voltage rms value for alternating current (ac) will determine the chopper switch, while the dc output voltage rms value will determine the unregulated rectifier. A direct current link capacitor is able to supply a constant direct current voltage to the chopper switch by reducing the amount of ripple that exists in the voltage that is generated by a rectifier. In other words, it smooths out the voltage. Any kind of disturbance in the waveform has the potential to cause damage to the switch. Where there is an abrupt switch ON and OF the controller the capacitor acts as a unresponsive short circuit for a momentary length of time through the transition. This is because of the rapid change. As a direct consequence of this, there is a possibility that the bridge rectifier may become faulty. As a result, a value of 4000 F is selected as a compromise in order to lower the charging current of the capacitor during the starting circumstances and also lower the wave content of the direct current voltage to a significant degree.

4) R_d Dump resistance

Calculating the assessment of R_d may be done as:

$$R_d = (V_{dc})^2 / P \text{ (W)} \quad (13)$$

As a result, if we retain the assessed power equal to 7500 W and the values of V_{dc} equal to 700V, we obtain R_d equal to 65. However, the accessible value of R_d for this control strategy has been decided to be 55 degrees.

2. CONTROL SCHEMES

5) Fuzzy Logic Control

In 1965, Zadeh was the first person to come up with the idea that would later become known as the fuzzy set theory. This theory serves as the basis for fuzzy logic control. The concept of fuzzy set theory is predicated on the premise that there is a changeable connection between membership and non-membership functions. As a consequence of this, the bounds or borders of fuzzy sets can at times be ambiguous and foggy, which is useful for the design of systems that include approximation. FLCs are a wonderful alternative to go with since they are easy to use and adaptable in their approach [12]. This makes them a terrific choice to go with when it is not viable to complete accurate mathematical formula calculations.

FLC is comprised of its four essential components, which are fuzziness, an understanding base, an interlocking system, and defuzzification. The AC voltage error, which is represented by the symbol e , and the change in error, which is

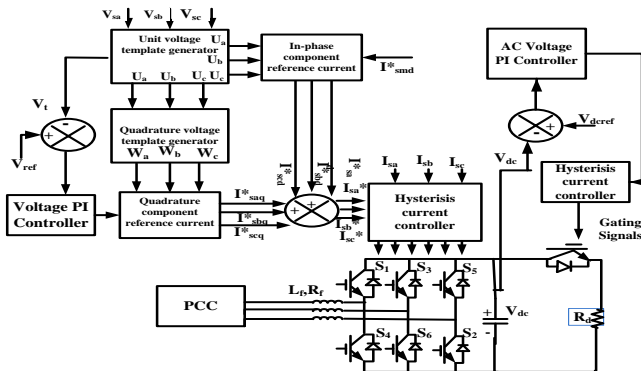


Fig.3 Schematic of a control strategy for SEIG electronic load controller using a proportional-integral controller

represented by the symbol ce , are the principal inputs of FLC. The input signals are sent to the fuzzification component, which then converts them into values with a fuzzy quality. The membership functions of these fuzzy values are given using the shape of the variables of fuzzy linguistic, who may also be thought of as fuzzy sets. An information that is essential to interpret linguistic descriptions that are stated through the lens of logical implications is stored in the knowledge base. The interference mechanism performs an analysis on the murky data and makes use of a predetermined set of control rules. After that, the input circumstances are placed through a defuzzification process, which uses a variety of different methods, including center of gravity, highest, and balanced mean, amongst others, in order to transform them into control signals. After that, these control indications are implemented into the system that is really being used. Before the input signals are handled by the fuzzy logic controller, they are first stated in fuzzy set notations via the use of linguistic labels that are characterized by membership grades.

Figure 3 presents an in-depth view of the FLC's structural makeup. Because of their symmetrical alignment along the axis, ease of implementation, and simplicity, triangle membership functions are favored in this fuzzy controller architecture. In accordance with the architecture of the FLC [13], the scaling factors G_e , G_{ce} , and G_u are used in the process of scaling the inputs and outputs. The errors "e" and "ce" at the nth sampling immediate, both of these are inputs to FLC and may be expressed as

$ce(n) \backslash e(n)$	NB	NM	NS	ZE	PS	PM	PM
NB	NB	NB	NB	NB	NM	NS	ZE
NM	NB	NB	NB	NM	NS	ZE	PS
NS	NB	NB	NM	NS	ZE	PS	PM
ZE	NB	NM	NS	ZE	PS	PM	PB
PS	NM	NS	ZE	PS	PM	PB	PB
PM	NS	ZE	PS	PM	PB	PB	PB
PB	ZE	PS	PM	PB	PB	PB	PB

$$e = V_{dref} - V_{dc} \tag{14}$$

$$ce(n) = e(n) - e(n-1) \tag{15}$$

The fuzzy logic controller adheres to the principles that are outlined in Table I, which may be found here. In this investigation, the max-min inference technique that was created by Mamdani is used to ascertain the values of an assumed fuzzy set of tuning rules. In order to clarify the control variables that were specified, the centroid methodology was ultimately chosen as the best option. [9-10,15]

TABLE I RULE BASE FOR FUZZY LOGIC CONTROLLER

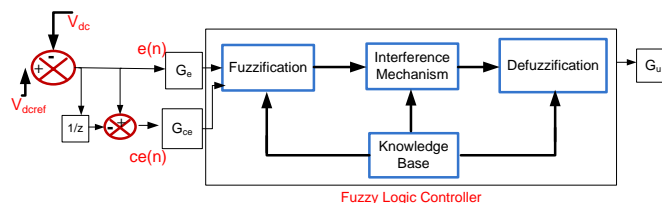


Figure.4. Fuzzy Logic Controller Structure

6) Proportional Integral Controller (PI)

The following equations are the ones that the PI controller uses as its working equations:

The inaccuracy in the ac voltage measured at the nth sampling moment, denoted as

$$V_{er(n)} = V_{tmref(n)} - V_{tm(n)} \tag{16}$$

where the amplitude of the reference ac terminal voltage is symbolized by the symbol $V_{tmref(n)}$, and the amplitude of the measured 3-phase ac voltage at the terminal of an induction generator at the nth sampling instant is symbolically represented by the symbol $V_{tm(n)}$, respectively.

To ensure that the ac terminal voltage remains unaltered at the nth sampling instant, the following formula is used to determine the value of the output of the PI controller, which is indicated by the symbol $I_{smq(n)}$:

$$I_{smq(n)} = I_{smq(n-1)} + K_{pv}\{V_{er(n)} - V_{er(n-1)}\} + K_{iv}V_{er(n)} \tag{17}$$

where K_{pv} and K_{iv} are the voltage proportional (PI) controller's integral and proportional gain constants, and 700V is assumed to be the value of V_{tref} .

The value of V_{dref} is chosen to be 600V, and the Zeigler-Nichols step response approach [4] is used to determine the proportional gains K_{pc} and K_{ic} associated with the voltage. After observing the step reaction of the open loop system, the highest gradient (G) and the moment at which this line of maximum gradient crosses the time axis (T) are calculated from this response. The size of the step response that is being applied is denoted by 'U,' and the advances of the PI controller are determined by utilizing these formulas:

$$K_{pc} = mod \{(1.2U/GT)\} \tag{18}$$

$$K_{ic} = mod \{(0.6U/(GT^2))\} \tag{19}$$

The value of the gains discussed above that are related with the voltage open loop system is provided in the appendix..

3.RESULTS AND DISCUSSION

The ELC for SEIG as well as its control techniques have been shown and simulated with the help of MATLAB and Simulink, and its functionality under a range of linear and nonlinear load conditions has been looked at. Waveforms of compensatory current (I_{cc}), the generator voltage (V_s), load current (I_{load}), DC link voltage (V_{dc}), generator current (I_s), excitation current (I_{ec}), and rotor speed and rotor frequency (m, f) are revealed in Figures 5 through 8, respectively. In addition, for the goal of contrasting fuzzy logic controllers with PI controllers, graphic representations of their

corresponding DC link voltages (Vdc) under both nonlinear and linear load scenarios are investigated. This is done in order to make a comparison between the two types of controllers. In the simulation, an induction machine with 4 poles, 7.5 kW of power, 415 V of voltage, and 14.8 A of current served as the induction generator. The appendix contains a detailed listing of the simulation's requirements for this induction generator.

B. Effectiveness of the SEIG-ELC with a Fuzzy Controller under Linear and Nonlinear Load

Fig. 5 shows an illustration of the efficiency of an ELC that is linked to a balanced reactive load and is controlled by a fuzzy logic controller. At 0.6 seconds, a 7.5-kilowatt balanced reactive load with 0.8 power factor (PF) is delivered to the system. The efficiency of the controller is shown by the fact that the ELC keeps the output voltage consistent during the whole process, therefore controlling both the voltage and the frequency. The efficiency of the SEIG device having a 6 kW resistant load applied at the Direct Current end of the three-phase unregulated rectifier is shown in Figure 6 under nonlinear load conditions. The nonlinear load is linked at 0.62 seconds and remains attached until the completion of the process. The level of Vdc, which had been steady, drops slightly for a few seconds but then recovers to its previous level at around 0.72 seconds later and remains stable until the conclusion of the experiment.

C. Effectiveness of SEIG-ELC while feeding 3-phase linear and nonlinear load with PI Controller system

Figure 7 is an illustration that shows how effectively the PI voltage control-based SEIG-ELC systems operate when it is linked to a linear reactive load. A balance reactive load of 7.5kW with 0.8PF lagging is attached at a time of 0.62sec and the voltage retains its uniformity through every component of the system. The functioning of this system is examined in Figure 8, which depicts the situation in which it is exposed to a nonlinear load. At the DC end of this system is a resistive load that is rated at 7.5 watts, which is part of a three-phase uncontrolled rectifier circuit that makes up this system. An additional nonlinear load is introduced into the system at a time period of 0.62 seconds. Throughout the duration of the simulation with power quality, it is noticed that both the voltage and the frequency stay steady.

D. Comparative analysis of Direct Current link voltage in SEIG-ELC system

A contrast of the direct current link voltage within the SEIG-ELC (Fuzzy logic control-based) system having a linear load and the SEIG-ELC (PI voltage control-based) network is shown in Figure 9. This comparison can be found in the same figure. In contrast to the PI control method, the fuzzy control approach requires a much shorter amount of time for the

settlement procedure to be completed. The amount of time required to stabilize the direct current link voltage in fuzzy control is shorter, and it also attains a bigger steady voltage than the PI control ensures. This occurs at the time when linear reactive load is delivered mutually both systems for 0.62 seconds. This transpires as a result of using the fuzzy control. It takes the PI control system little under 0.85 seconds to reach a degree of stability after the dc link voltage has been stabilized. Figure 10 provides a visual representation of a comparison between the two distinct control systems in the nonlinear load condition context. The direct current link voltage which is associated with fuzzy control stabilizes at nearly 0.7 seconds whenever the nonlinear load is attached at a time of 0.62 seconds. When compared to the settlement period of 0.8 seconds that is associated with PI control, this length of time is much shorter. As a result of these results, one can draw the conclusion which provide the fuzzy logic controller-based SEIG-ELC mechanism is preferable than the PI control system in terms of its capacity to regulate voltage. This conclusion may be supported by the fact that the fuzzy logic controller-based SEIG-ELC mechanism.

4.CONCLUSIONS

As a consequence of this, the present work offers two efficient control techniques for an SEIG that is driven by a constant power. The many results that were provided above suggest that the control scheme has been effective in regulating voltage and frequency in linear as well as nonlinear load situations. This is shown by the fact that the system was successful in being presented above. This is proved by the fact that the control scheme has been shown to be effective. Under a variety of electrical load circumstances, the performance of SEIG is improved by the suggested ELCs, as well as its control systems, which also offer reactive power compensation for SEIG. The controllers offer excellent performance in terms of feeding power to balanced load circumstances for an isolated power generating system. The controllers have powerful load leveling capabilities, in addition to their ability to keep the voltage and frequency levels consistent. The results of the research done on the steady state indicate that the ELC that is controlled by fuzzy logic is superior than the ELC that is controlled by proportional integral.

5.APPENDIX

a. Data of SEIG

The following is a breakdown of the specifications for an induction machine with 4 poles, 7.5 kW of power, 415 volts, and 50 hertz:

$$R_s = 1\Omega, R_t = 0.77\Omega, X_{lt} = X_{ls} = 1.5\Omega, J = 0.1384 \text{ kg} - \text{m}^2$$

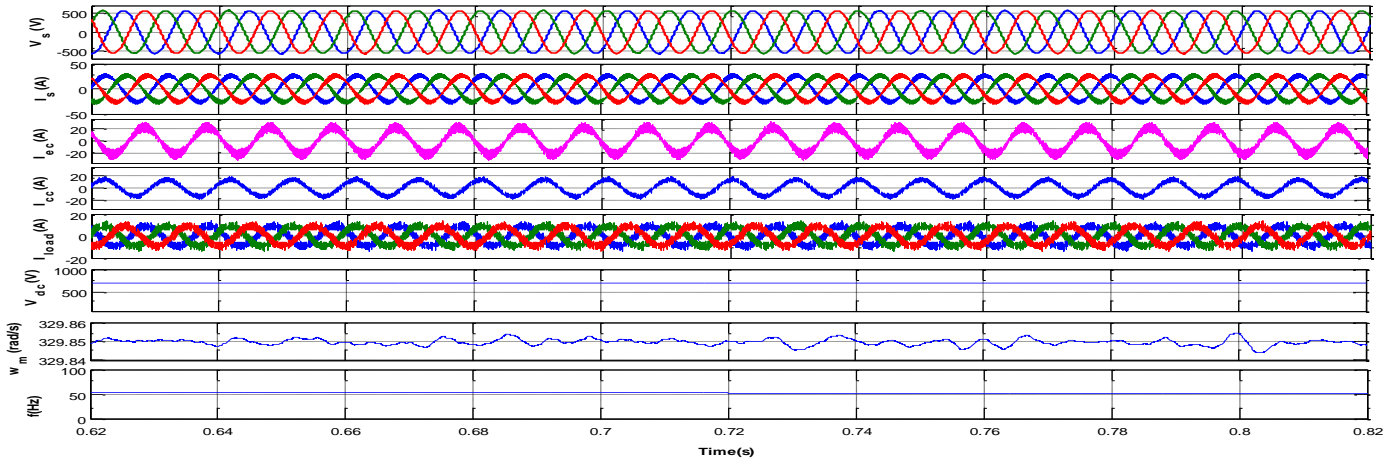


Fig.5. 7.5 kW SEIG waveforms feeding linear reactive load with fuzzy logic control-based ELC

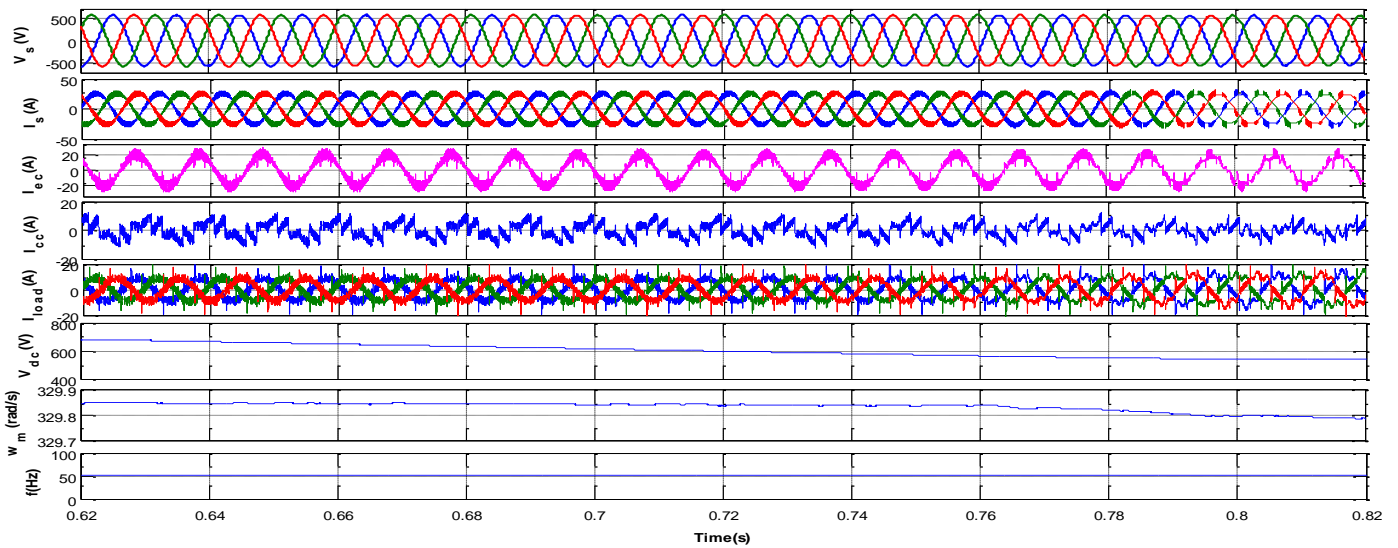


Fig.6. SEIG Waveforms with Fuzzy Logic Control-based ELC Feeding Nonlinear Load

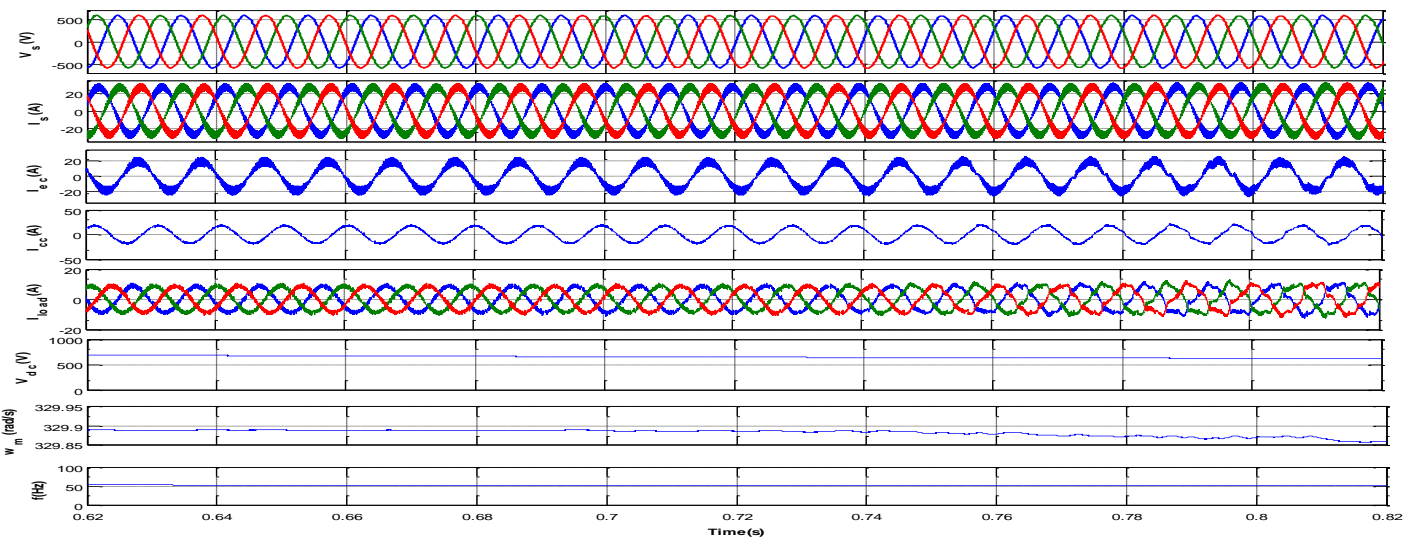


Fig.7. SEIG voltage control-based ELC waveforms supporting a 7.5 kW linear load

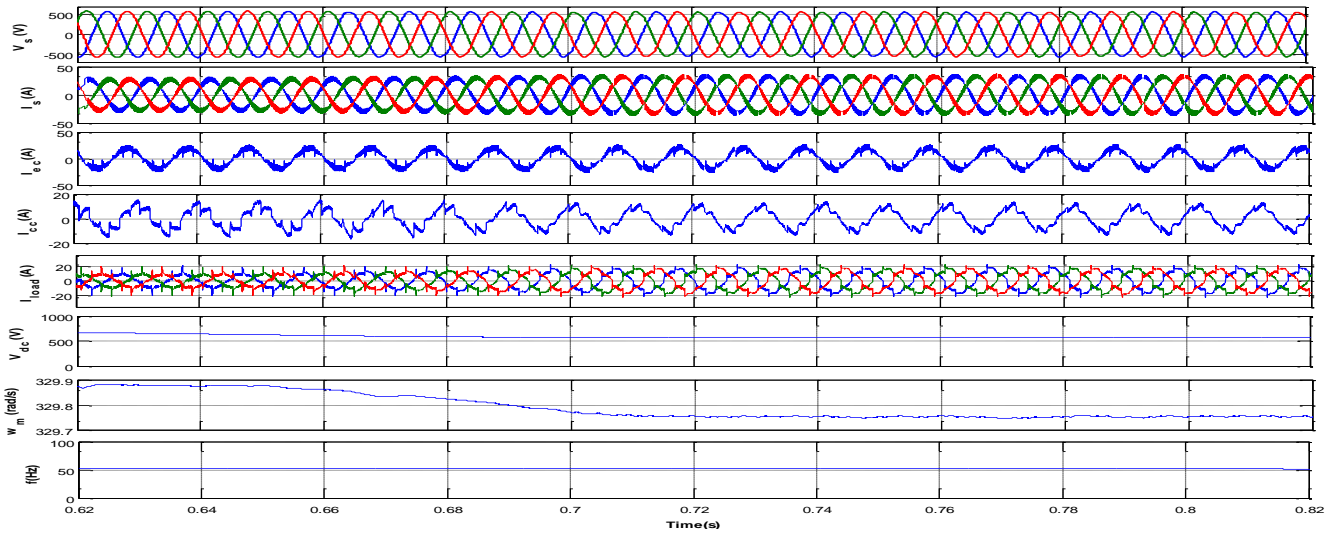


Fig.8. SEIG waveforms supplying a nonlinear load using an ELC based on PI voltage control.

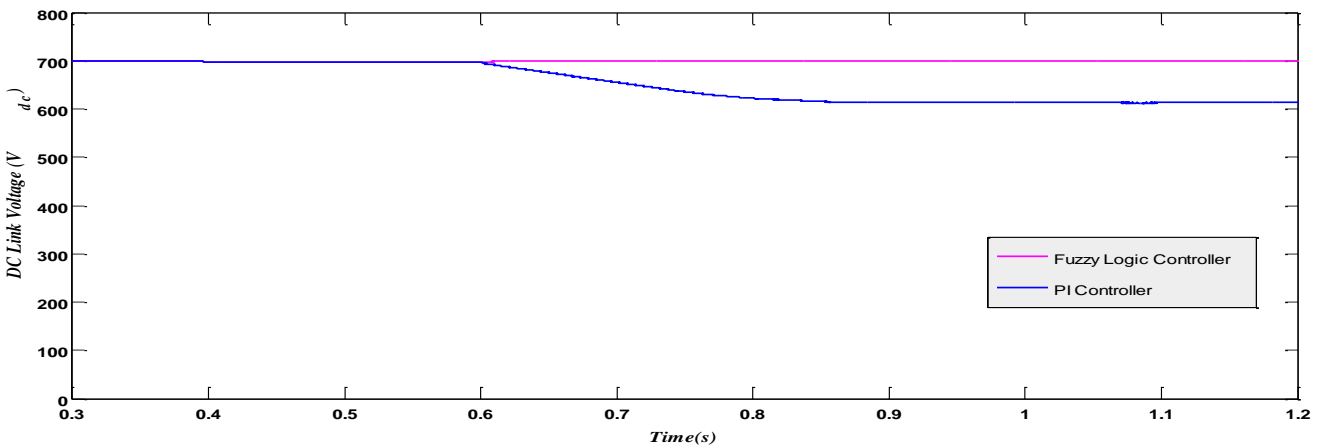


Fig. 9 SEIG-ELC system delivering linear load: comparison of direct current link voltage for the fuzzy logic controller and PI controller

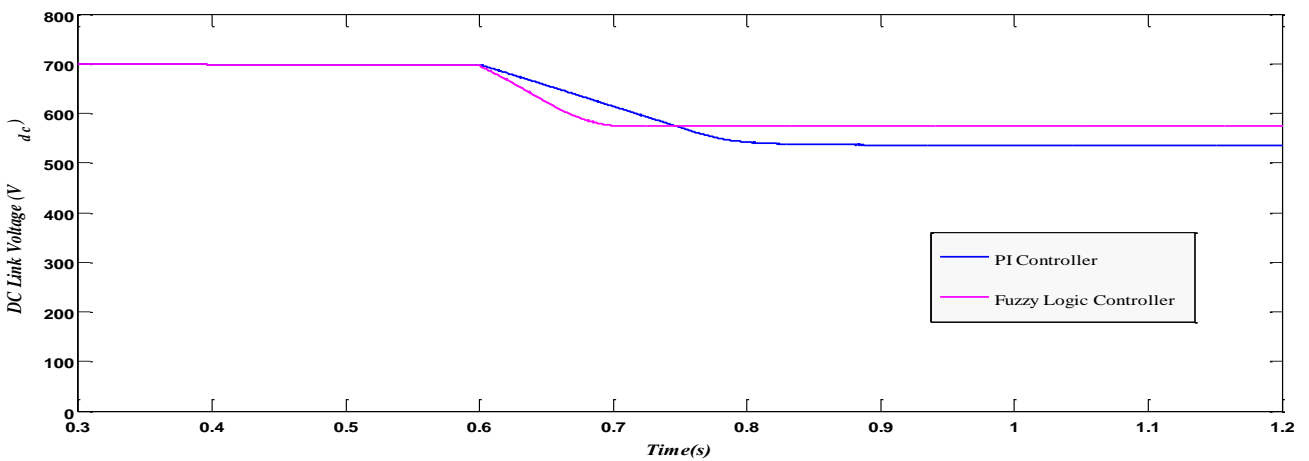


Fig. 10 Fuzzy logic controller and PI controller comparison for the SEIG-ELC system delivering a nonlinear load

b. Controller constraints

$$L_f = 1.2mH, R_f = 0.06\Omega \text{ and } C_{dc} = 4000\mu f, R_d = 55\Omega$$

For the Alternating Current PI voltage controller, $K_{pv} = 0.16, K_{iv} = 0.14$

For DC link Capacitor voltage PI Controller, $K_{pc}=1.98, K_{ic}= 0.001$

C. The Loads of the Consumers

The inertia of reaction 7.5 kilowatts of trailing three-phase loads at 0.8 percent power factor

Load that is nonlinear 6 kW at the direct current end of the 3-phase diode rectifier

c. Prime Mover Features

$$T_{sh} = K_1 - K_2\omega_r, K_1 = 3300, K_2 = 100$$

6. REFERENCE

[1] R.C. Bansal, "Three-phase Self-excited induction generators: An Overview", *IEEE Transc. On Energy Conversion*, vol. 20, no. 2, pp. 292-299, June 2005.

[2] Bhim Singh and Gaurav Kumar Kasal, "Solid state voltage and frequency controller for a standalone wind power generating system", *IEEE Transc. On power electronics*, vol. 23, no. 3, May 2008.

[3] Bhim Singh and Gaurav Kumar Kasal, "Voltage and frequency controller for isolated Asynchronous generators feeding 3-phase 4-wire Loads", *IEEE*, 2006.

[4] Bhim Singh and Gaurav Kumar Kasal, "Solid state controller for an isolated wind energy conversion system feeding dynamic loads", *The 8th International Power Engineering Conference*, 2007.

[5] Bhim Singh, Gaurav Kumar Kasal, Ambrish Chandra, Kamal-Al—Haddad, "Electronic load controller for parallel operated Isolated asynchronous generators feeding various loads", *Journal of Electromagnetic Analysis and Applications*, 2011.

[6] Bhim Singh, S.S. Murthy and Sushma Gupta, "STATCOM based voltage regulator for self-excited induction generator feeding nonlinear loads", *IEEE Transc. On industrial electronics*, vol. 53, no. 5, Oct 2006.

[7] Dandan Ma, "Self-excited induction generator – A study based on nonlinear dynamic methods", *School of Electrical and Electronics, NewCastle University, U.K*, May 2012.

[8] Ambarnath Banerji, Sujit K. Biswas and Bhim Singh, "Voltage and frequency controllers for an autonomous asynchronous generator", *International Journal on Electrical Engineering and Informatics*, vol. 6, no. 2, June 2014.

[9] Yahya Sofian, Munawar Iyas, "Design of Electronic load controller for Self excited induction generator using Fuzzy logic based microcontroller", *International Conference of Electrical Engineering and Informatics*, July 2011.

[10] Sarsing Gaoy, S.S. Murthy, G. Bhuvaneswari, and M. Sree Lalitha Gayathri, "Design of microcontroller based Electronic load controller for a Self excited induction

generator supplying single-phase loads", *Journal of Power Electronics* vol 10, no. 4, July 2010.

[11] Bhim Singh, Ambrish Chandra, Kamal-Al—Haddad, "Harmonic elimination, reactive power compensation and load balancing in three phase, four wire electric distribution systems supplying nonlinear loads", *Journal of Electric Power system Research, Elsevier*, Febraury 1998.

[12] Karuppanan P and KamalaKanta Mahapatra, "PLL with Fuzzy logic controller based shunt active power filter for harmonic and reactive power compensation", *IEEE*, 2011.

[13] Nitin Gupta and S. P. Singh, "Fuzzy logic controlled shunt active power filter for reactive power compensation and harmonic elimination", *International Conference on Computer and Communication Technology*, 2011.

[14] Yogesh K. Chauhan, Sanjay K Jain and Bhim Singh, "A prospective on voltage regulation of Self-excited induction generators for industry applications", *IEEE Transc. On Industry Applications*, vol. 46, no. 2, March 2010.

[15] C. Kathirvel, Dr. K Porkumaran, "Fuzzy logic based voltage and frequency for Self excited induction Generator for micro hydro turbines for rural applications", *Journal of Theoretical and Applied Information and Technology*, vol 54, no.1, August 2013.